Methylene blue not ferrocene: Optimal reporters for electrochemical detection of protease activity

Biosensors and Bioelectronics ■ (■■■■) ■■■–■■■

Contents lists available at ScienceDirect

Biosensors and Bioelectronics

journal homepage: www.elsevier.com/locate/bios

Methylene blue not ferrocene: Optimal reporters for electrochemical detection of protease activity

Eva González-Fernández [a,1], Nicolaos Avlonitis [a,1], Alan F. Murray [b], Andrew R. Mount [a,*], Mark Bradley [a,*]

[a] EaStCHEM, School of Chemistry, University of Edinburgh, Joseph Black Building, West Mains Road, Edinburgh EH9 3FJ, UK
[b] School of Engineering, Institute for Bioengineering, The University of Edinburgh, The King's Buildings, Mayfield Road, Edinburgh EH9 3JL, UK

ARTICLE INFO

Article history:
Received 30 September 2015
Received in revised form
24 November 2015
Accepted 27 November 2015

Keywords:
Methylene blue-tagged peptides
Self-assembled monolayer
Electrochemical detection
Protease detection
Clinically-relevant protease sensing

ABSTRACT

Electrochemical peptide-based biosensors are attracting significant attention for the detection and analysis of proteins. Here we report the optimisation and evaluation of an electrochemical biosensor for the detection of protease activity using self-assembled monolayers (SAMs) on gold surfaces, using trypsin as a model protease. The principle of detection was the specific proteolytic cleavage of redox-tagged peptides by trypsin, which causes the release of the redox reporter, resulting in a decrease of the peak current as measured by square wave voltammetry. A systematic enhancement of detection was achieved through optimisation of the properties of the redox-tagged peptide; this included for the first time a side-by-side study of the applicability of two of the most commonly applied redox reporters used for developing electrochemical biosensors, ferrocene and methylene blue, along with the effect of changing both the nature of the spacer and the composition of the SAM. Methylene blue-tagged peptides combined with a polyethylene-glycol (PEG) based spacer were shown to be the best platform for trypsin detection, leading to the highest fidelity signals (characterised by the highest sensitivity (signal gain) and a much more stable background than that registered when using ferrocene as a reporter). A ternary SAM (T-SAM) configuration, which included a PEG-based dithiol, minimised the non-specific adsorption of other proteins and was sensitive towards trypsin in the clinically relevant range, with a Limit of Detection (LoD) of 250 pM. Kinetic analysis of the electrochemical response with time showed a good fit to a Michaelis–Menten surface cleavage model, enabling the extraction of values for k_{cat} and K_M. Fitting to this model enabled quantitative determination of the solution concentration of trypsin across the entire measurement range. Studies using an enzyme inhibitor and a range of real world possible interferents demonstrated a selective response to trypsin cleavage. This indicates that a PEG-based peptide, employing methylene blue as redox reporter, and deposited on an electrode as a ternary SAM configuration, is a suitable platform to develop clinically-relevant and quantitative electrochemical peptide-based protease biosensing.

1. Introduction

Proteases are enzymes that catalyse the cleavage of amide bonds at specific sites in a protein or peptide. Among their myriad of physiological roles, these enzymes are involved in many pathophysiological conditions, including inflammation and cancer (Li and Yuan, 2008; Mason and Joyce, 2011; van Kempen et al., 2006). Hence, there is an increasing demand for selective, sensitive and miniaturised analytical tools for the analysis of protease function/activity in a biomedical setting.

Peptide-based biosensors for protein detection (i.e. proteases, kinases, antibodies, etc.) have been successfully developed, based on the conjugation of a relevant peptide sequence to a signal reporter (e.g., fluorophore, nanoparticle, redox tag) that are then able to generate a measurable output upon recognition of the target analyte (Liu et al., 2015; Pavan and Berti, 2012; Pazos et al., 2009). Electrochemical biosensors that utilise peptide probes labelled with a redox active moiety have proven to be valuable tools for the detection of proteins such as proteases (Anne et al., 2012; Kerman et al., 2007; Xiao et al., 2008), including matrix metalloproteinases (MMPs) (Liu et al., 2006; Shin et al., 2013), HIV-1 reverse transcriptase (Labib et al., 2011) or antibodies (Puiu et al., 2014). Electrochemical protease detection has been achieved using peptide-based sensors consisting of redox-labelled peptide probes immobilised onto an electrode surface that are then cleaved by the

* Corresponding authors.
E-mail addresses: a.mount@ed.ac.uk (A.R. Mount), mark.bradley@ed.ac.uk (M. Bradley).
[1] These authors contributed equally to this study.

http://dx.doi.org/10.1016/j.bios.2015.11.088
0956-5663/

target enzyme (Anne et al., 2012; Liu et al., 2006; Shin et al., 2013; Xiao et al., 2008; Zhao et al., 2010), with the enzymatic activity being measured by the signal decrease on the electrode arising from the loss of the redox-labelled probe fragment from the surface due to enzymatic cleavage.

Probe design requires modification of the peptide via the addition of a redox reporter at one end and an anchoring thiol-containing moiety for attachment to the gold electrode at the other. A spacer unit is typically added to ensure the peptide-probe sequence is sufficiently far away from the gold surface to enable enzyme binding and peptide cleavage. Clearly these various modifications will have an impact on a biosensor's performance. The majority of peptide-based electrochemical sensors use ferrocene (Fc) (Anne et al., 2012; Kerman et al., 2007; Liu et al., 2006; Martić et al., 2011; Xiao et al., 2008) as the redox reporter; and although methylene blue (MB) (Puiu et al., 2014; Shin et al., 2013) has also been used for this purpose, there are far fewer examples in the literature. Fc and MB both benefit from ease of conjugation to the peptide probe, they also show electrochemically reversible redox behaviour, and have therefore also been widely used as reporters in other electrochemical sensor probes including DNA (Lubin and Plaxco, 2010) and aptamers (White et al., 2010). Differences in performance have been reported depending on the redox reporter used (Ferapontova et al., 2008; Kang et al., 2009), while the spacer connecting the peptide sequence and the anchor moiety in combination have also been shown to play an important role in the electrochemical performance of these sensors (Henry et al., 2010; Lai et al., 2006; Phares et al., 2009).

Electrochemical detection platforms benefit from a fast response, ease of miniaturisation (allowing the development of point-of-care devices), minimal sample preparation and high sensitivity and selectivity (Ferapontova et al., 2008; Lai et al., 2007; Wang, 2006). Alongside these advantages, there are also important challenges, including significant non-specific binding, in which non-sequence specific interactions of species other than the target with the probe layer leads to false positive signals and/or reduced sensitivity. The composition and structure of the modified surface dramatically affect this biosensor performance. Typically, the developed sensing phases consist of mixed self-assembled monolayers (SAMs) comprising a bio-recognition element (probe), and a backfilling molecule (typically mercaptohexanol), which is thought to help the orientation (and hence accessibility) of the probe sequence and avoids pin-holes in the SAM structure (and hence non-specific adsorption to the underlying electrode). Extensive work has also been carried out to improve the anti-fouling (the inhibition of non-specific binding to the probe film surface) capability of SAMs for enhanced electrochemical detection. This includes the so-called ternary SAM (T-SAM) films, which employ a third component, such as dithiols (Campuzano et al., 2011; Campuzano et al., 2012; Wu et al., 2010), charged components like 3-mercaptopropionic acid (Dharuman et al., 2010), thiolated-ethyleneglycols (Henry et al., 2010) or thiolated oligonucleotides (McQuistan et al., 2014) to add this capability.

Herein we report on the systematic tuning of peptide-based probes and SAM structure for enhanced electrochemical protease biosensing with direct side-by-side evaluation of the effect of two different redox tags (Fc, MB), the influence of the nature of the spacer connecting the peptide sequence to the anchor moiety, and the development of a new ternary SAM platform consisting of a PEG-based dithiol as a third component, which tailors the surface properties for optimal target accessibility whilst blocking the non-specific adsorption of proteins.

2. Materials and methods

2.1. Instrumentation

Electrochemical measurements were performed using a conventional three-electrode electrochemical cell driven by a computer-controlled AutoLab PGstat-30 potentiostat running the GPES 4.9 software (EcoChemie, The Netherlands). A platinum wire and a 2 mm diameter polycrystalline gold electrode (IJ Cambria, UK) were used as auxiliary and working electrode, respectively. All the potentials are referred to the Ag|AgCl|KCl (3 M) reference electrode (Bioanalytical Systems, Inc., USA).

2.2. Reagents and experimental methods

The source of all reagents and the experimental methods are described in Supplementary Data.

3. Results and discussion

In the present work an electrochemical biosensor for protease detection based on the immobilisation on a gold surface in a SAM of a short redox-labelled peptide sequence containing a specific cleavage site is presented. This SAM-modified surface was electrochemically interrogated before and during exposure to enzyme, which causes enzyme-catalysed cleavage and release of the redox reporter-containing fragment into solution. This led to the progressive decrease of the peak current measured by SWV, with the fraction of cleaved peptide being given by the fractional decrease of the peak redox signal from that registered before enzyme addition (the arrow in Fig. 1). It should be noted that although Fig. 1 suggests the principle of detection is direct through-space electron transfer between electrode and extended peptide, this is extremely unlikely, given the distances involved. Some authors have suggested significant electron transfer through the peptide backbone (Puiu et al., 2014; Shah et al., 2015), but an alternative, and likely dominant, electron transfer mechanism arises from the facile bending of the flexible peptide probe, which enables the redox tag to approach close enough to the electrode surface to facilitate rapid electron transfer. The exact proportion of peak redox signal that originates from each of these mechanisms is immaterial, however, given the fact that peak signal reduction results from

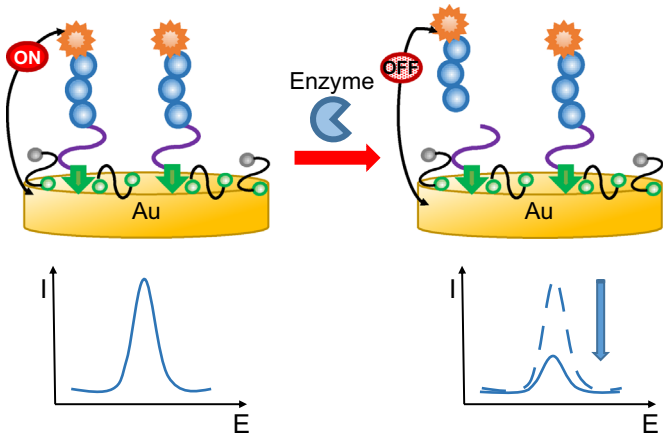

Fig. 1. Principle of detection of the peptide-based electrochemical sensor for protease detection. The peptide sequence Phe–Arg–Arg is conjugated to a redox tag at one end and a spacer with an anchor moiety (cysteine) at the other and this is attached to a gold surface. The presence of the protease (trypsin) catalyses the cleavage of the peptide sequence releasing the redox-containing fragment into solution.

Please cite this article as: González-Fernández, E., et al., Biosensors and Bioelectronics (2015), http://dx.doi.org/10.1016/j.bios.2015.11.088

Table 1
Composition and structure of peptides and sensing phases used throughout this work. Details of the synthetic methods and peptide characterisation data are to be found in the Supplementary Data.

Compound	Peptide sequence	Structure
Peptide-1	Fc-FRR-Ahx-C-NH_2	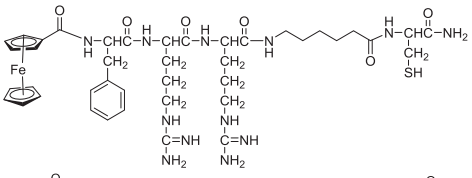
Peptide-2	Fc-frr-Ahx-C-NH_2	
Peptide-3	Fc-FRR-PEG-C-NH_2	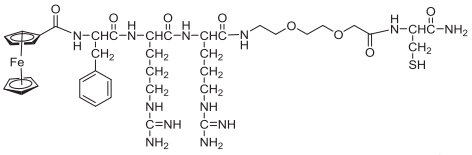
Peptide-4	Fc-frr-PEG-C-NH_2	
Peptide-5	MB-FRR-PEG-C-NH_2	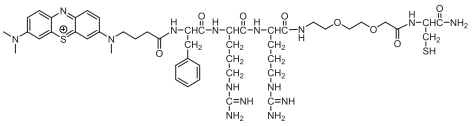
Peptide-6	MB-frr-PEG-C-NH_2	
Sensing phase	**Composition**	**Schematic composition**
B-Peptide-1	Peptide-1 + MCH	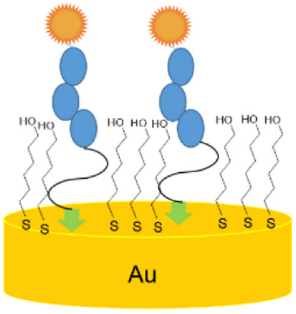
B-Peptide-2	Peptide-2 + MCH	
B-Peptide-3	Peptide-3 + MCH	
B-Peptide-4	Peptide-4 + MCH	
T-Peptide-3	Peptide-3:HDT + MCH	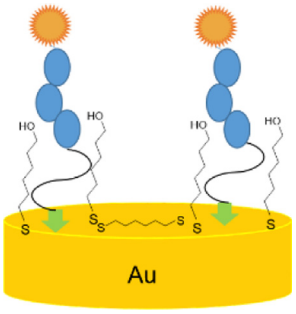
T-Peptide-4	Peptide-4:HDT + MCH	
T-Peptide-5	Peptide-5:HDT + MCH	
T-Peptide-6	Peptide-6:HDT + MCH	
T-PDT-Peptide-5	Peptide-5:PDT + MCH	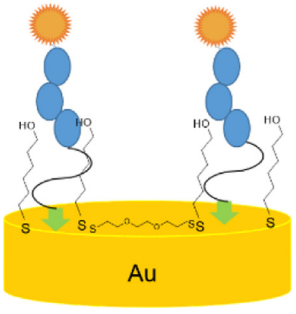
T-PDT-Peptide-6	Peptide-6:PDT + MCH	

Ahx: 6-aminohexanoic acid, PEG: 8-amino-3,6-dioxaoctanoic acid, Fc: ferrocene, MB: methylene blue F = L-Phenylalanine, R = L-Arginine, f = D-Phenylalanine, r = D-Arginine, MCH: 6-mercaptohexanol, HDT: 1,6-hexanedithiol, PDT: 2,2'-(ethylenedioxy)diethanethiol.

Please cite this article as: González-Fernández, E., et al., Biosensors and Bioelectronics (2015), http://dx.doi.org/10.1016/j.bios.2015.11.088

probe cleavage. However, the latter mechanism does indicate one potential role for other components in the B-SAM and T-SAM systems, as these will modify the interfacial properties of the electrode and hence the degree to which redox reaction will occur.

Different redox-tagged peptides were designed and synthesised. Two modifications were introduced: a redox tag (Fc or MB) at the amino-terminus and a spacer (an alkyl or PEG-based chain), with a cysteine moiety at the carboxy-terminus which enables peptide attachment onto a gold surface through the thiol group. In all cases the equivalent uncleavable D-amino acid based probes were also synthesised, to constitute a negative control (Table 1). Comparison of probes as sensing agents was carried out by producing thiol-modified peptide probe SAMs and evaluating their stability and performance upon the addition of trypsin. One role for the alkyl or PEG-based chain is that of spacer between the cysteine anchor and the peptide sequence. The concept was to both make the cleavage site more available to the enzyme by bringing it away from the gold surface and to enhance the flexibility of the probe, to improve sensitivity through increasing both the degree of enzyme cleavage (loss of signal) and the peak current (signal) registered by SWV due to enhancement of the dominant electron transfer mechanism. A further role, arising from their chemical difference, may be to enable some tuning of the structure, composition and resulting sensing properties of the SAM.

3.1. Effect of the spacer

Probes were designed and synthesised, consisting of a peptide sequence modified at both amino- and carboxy-terminii; with a Fc moiety and an aminohexyl (Ahx) or a PEG-based chain attached to a cysteine moiety and the appropriate L- or D- amino acids (Table 1). The sensing phase consisted of a mixed B-SAM comprising the immobilised peptide probe (formed by overnight incubation with a 20 μM solution of the selected peptide prepared in ethanol at 4 °C) followed by a backfilling step with MCH (1 mM in ethanol, 1 h at room temperature) to fill any exposed gold patches or pin-holes, to give the two sensing phases B-Peptide-1 and B-Peptide-3 and their control phases B-Peptide-2 and B-Peptide-4 respectively (Table 1). Each of the four modified surfaces was then immersed in a 1x PBS solution containing 0.6 M $NaClO_4$ and subjected to successive electrochemical SWV measurements for 50 min, which typically resulted in a steady (overall 5–10%) decrease in the peak registered in all cases (which can be considered to be the change in redox signal with time). After the addition of trypsin to give a final concentration of 30 μM the signal was monitored for a further 40 min. The rate of signal decrease recorded after trypsin addition was the same within experimental error for both B-Peptide-1 and B-Peptide-2 surfaces (with the alkyl spacer), suggesting the enzyme was not able to bind to the recognition site and turn-over to release the redox-tagged fragment in either case. On the other hand, B-Peptide-3 (containing the PEG spacer and the L-amino acid peptide) showed a significantly increased rate of signal loss, with an overall ~25% decrease in signal. That this was due to release of the redox tag from the substrate-modified surface (B-Peptide-3) due to protease cleavage was confirmed by the fact that only a ~5% decrease was seen for the B-Peptide-4 surface (which has a PEG spacer and an identical D-amino acid peptide sequence). It can be concluded that the PEG-based spacer is crucial in enabling effective cleavage. PEG chains are known to increase hydrophilicity of a material or surface, promoting mobility and biomolecular interactions (Charles et al., 2009). Another possible explanation for this effect is that the PEG-based chain spacer is highly solvated allowing the formation of a less packed SAM interior, giving greater spacing between immobilised probes on the gold surface, and enhancing enzyme access compared to the more packed SAMs obtained for the alkyl chain spacer.

3.2. Effect of probe spacing through changing the SAM configuration: binary vs ternary

Two different SAM configurations were prepared for each of the probes Peptide-3 and Peptide-4. B-Peptide-3 and B-Peptide-4 were prepared and an analogous T-SAM was prepared for each probe by the introduction of a dithiol (HDT) as the third component (Table 1). These sensing phases were subjected to SWV measurements in 1x PBS. A percentage signal decrease of around 5–10% was registered after 40 min for all the four SAM types tested, which was consistent with the B-SAM measurements (see Section 3.1) and again indicates background redox signal stability as a function of time and similar initial behaviour for B-SAM and T-SAM films. Four successive trypsin additions were then carried out (to give final concentrations of 30, 60, 90 and 120 nM), with the electrochemical signal monitored by SWV for a further 30 min between each addition. The uncleavable Peptide-4-modified surfaces showed an overall percentage signal decrease of just ~7%, allowing us to conclude that the change in the SAM configuration from B- to T- did not affect the non-specific interaction of trypsin.

In contrast, the Peptide-3-modified surfaces showed signal decreases of ~15% for B-Peptide-3, and ~25% for T-Peptide-3. To explain the enhanced T- signal decrease, it is postulated that the introduction of the dithiol produces a more dilute surface, in terms of bound probe surface concentration, when compared to the B-SAM. The dithiol is also known to adopt a collapsed conformation with respect to the gold surface (Campuzano et al., 2011; Campuzano et al., 2012; Wu et al., 2010), thereby further increasing the spacing between probes and enabling higher enzyme accessibility and enhanced probe cleavage. Finally, it is worth noting that this change does not merely increase the rate at which probe is cleaved, but also the proportion of cleavable probes. The addition of dithiol therefore appears to lead to a greater proportion of probes which are cleavable by the enzyme.

3.3. Effect of redox label: Fc vs MB

In order to analyse and determine the optimal redox label, a side-by-side comparison was carried out on identical films prepared using Fc- and MB-tagged peptides. T-SAMs were prepared for all four peptide sequences (3-6) (Table 1). Fc-based SAMs (T-Peptide-3 and T-Peptide-4) showed a decrease of the registered signal of ~10% (Fig. 2A) with time, similar to previous data (Section 3.2). However, a stable signal was registered with time for MB-based SAMs (T-Peptide-5 and T-Peptide-6) (Fig. 2B), suggesting the difference was not due to differences in the rate of loss of peptide from the SAM (consistent with this rate of loss being insignificant, as expected due to the strength of the gold-thiol bond), but rather differences in stability of the redox label, as it undergoes repeated electrochemical redox cycling during SWV. Use of MB therefore essentially removes the unwelcome background signal decrease. That this is not at the loss of detection sensitivity and selectivity is demonstrated by the fact that subsequent trypsin addition produced a significant signal decrease recorded for the MB-substrate modified surface (T-Peptide-5) whilst a stable signal was recorded for the MB-control modified surface (T-Peptide-6). In contrast, the Fc-tagged peptide SAM T-Peptide-3 showed a similar decrease of signal upon trypsin addition, but with an additional significant contribution from background signal decrease (~20%) as shown by the Fc-modified control SAM surface, T-Peptide-4. These data suggest that the MB-based probes form SAMs with more stable electroactivity, able to generate more robust and readily analysable data for protease detection, free from the

Please cite this article as: González-Fernández, E., et al., Biosensors and Bioelectronics (2015), http://dx.doi.org/10.1016/j.bios.2015.11.088

complications of background drift. This is in agreement with previously reported results for electrochemical genosensors, where the ability of MB- and Fc-tagged ssDNA to form a SAM and act as a sensing phase for DNA detection was compared, which showed that MB-based SAMs led to a more stable sensing phase. This effect is attributed to the susceptibility of the oxidised form of ferrocene, ferrocinium Fc^+, to lose a ligand or to suffer an irreversible change in the electrochemistry due to nucleophilic attack (Kang et al., 2009). Overall it can be concluded that MB is a more robust electrochemical reporter than Fc.

3.4. Methylene blue-tagged peptides SAMs for trypsin detection

3.4.1. Optimisation of co-adsorbed Peptide-5:dithiol ternary SAM

Based on the data shown in Section 3.3, MB-tagged peptides in a T-SAM configuration were selected as the best molecular recognition configuration for developing an electrochemical sensor for detection of trypsin's proteolytic activity.

As previously reported, both surface coverage and inter-probe spacing play key roles in the analytical performance of electrochemical biosensors and these depend on the co-adsorbed dithiol concentration in T-SAMs (Campuzano et al., 2011). These properties were specifically optimised to obtain an enhanced signal by rational variation of the MB-tagged peptide/dithiol ratio ([Peptide-5]:[HDT]).

Different sensing phases were prepared following the two-step procedure described in Section S1.4 and using varying [Peptide-5]:[HDT] ratios as detailed in Section S1.5. Fig. 3 shows the percentage signal decrease registered for each ratio tested. Below 150 μM HDT, increasing the HDT concentration used for preparing the T-SAM translated into an increase of the signal loss. This is consistent with probe dilution in the T-SAM leading to an increased spacing between, and available proportion of, MB-tagged peptide probes, promoting the proportion of cleavable peptides and sensor sensitivity. However, from 150 to 900 μM the percentage signal decrease did not appear to vary within experimental error. The ratio of [Peptide-5] 40 μM:[HDT] 600 μM was therefore selected as optimum for further experiments. A further analysis of the effect on probe density of varying the concentration of HDT was also carried out by determining the redox-active peptide coverage on the electrode from the charge under the redox peak (see Section S2 and Fig. S1, Supplementary Data). This showed that the optimum ratio corresponded to a surface coverage of 2.3×10^{-12} mol/cm^2, and was consistent with the percentage signal decrease, with little variation in coverage between 150 and 900 μM HDT.

3.4.2. Effects of non-specific binding

The effect of non-specific binding on sensor response was investigated by monitoring the SWV signal upon addition of 100 nM BSA for T-Peptide-5 and T-Peptide-6. Fig. 3B depicts a signal decrease comparison for both types of SAM surface upon the addition of 100 nM trypsin (grey columns) and 100 nM BSA as a non-specific protein (hatched columns). It is clear that the T-SAM prepared with 600 μM HDT exhibited an undesired signal decrease upon the addition of 100 nM BSA for both substrate and control-modified surfaces (T-Peptide-5 and T-Peptide-6). These data are consistent with non-specific adsorption of BSA onto the modified surface, which reduces probe flexibility, prevents the redox tag approaching the electrode surface and thus translates into a decrease of the SWV signal. In order to overcome this problem T-SAMs were prepared using a PEG-based dithiol (PDT) instead of the alkyl-based dithiol (HDT) used previously, which showed markedly reduced signal decrease from non-specific binding (Fig. 3B). The resulting T-PDT-Peptide-5 sensing phase (Table 1) produced a slightly reduced, but still comparable, signal gain to the HDT analogue upon addition of trypsin (100 nM) (Fig. 3B, grey columns). Reassuringly, the control-modified surface (T-PDT-Peptide-6) also did not generate a significant signal upon trypsin addition. This confirms the potential of this T-SAM configuration, which includes a PEG-dithiol as a co-adsorbent, in enabling the detection of enzymatic activity whilst minimising the non-specific adsorption of proteins.

3.4.3. Quantitative electrochemical protease sensing

The optimised T-SAM MB-tagged peptide configuration (T-PDT-Peptide-5) was investigated as the basis of an electrochemical sensor for quantitative trypsin detection by immersion in solutions containing varying trypsin concentrations (0.1–100 nM) for 70 min. The electrochemical signal was monitored in real-time by SWV and again plotted as a percentage signal decrease (Fig. 4A).

For the lowest trypsin concentration tested (100 pM), a decrease of the signal of approximately 7% was recorded, which was still clearly distinguishable from the blank (0 nM trypsin). As depicted in Fig. 4, the higher the trypsin concentration in solution, the faster the percentage signal decrease registered, which is consistent with a more rapid proteolytic cleavage of the MB-tagged peptides immobilised onto the gold surface. The percentage decrease signal reached a saturation value for trypsin concentrations higher than 25 nM after 40 min. A negative control was performed by incubating 100 nM trypsin with T-PDT-Peptide-6 (Fig. 4), which was seen to be identical to the blank (T-PDT-Peptide-5 with no enzyme), further confirming the specificity of the sensing platform.

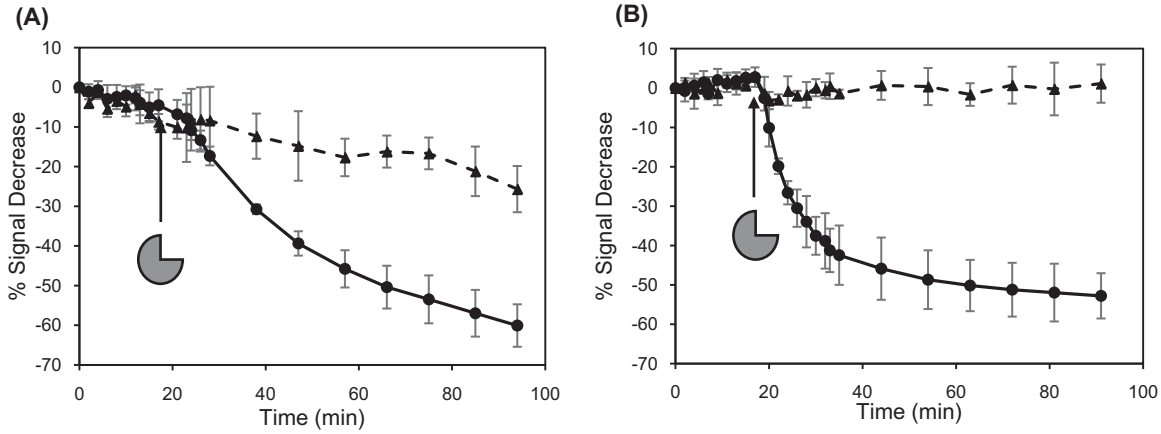

Fig. 2. Percentage signal decrease registered upon trypsin addition (100 nM) for (A) Fc-tagged peptides: T-Peptide-3 (circles) and T-Peptide-4 (triangles) and (B) MB-tagged peptides: T-Peptide-5 (circles) and T-Peptide-6 (triangles). All points and error bars represent the average of the response from at least 3 individual sensing SAM layers.

Please cite this article as: González-Fernández, E., et al., Biosensors and Bioelectronics (2015), http://dx.doi.org/10.1016/j.bios.2015.11.088

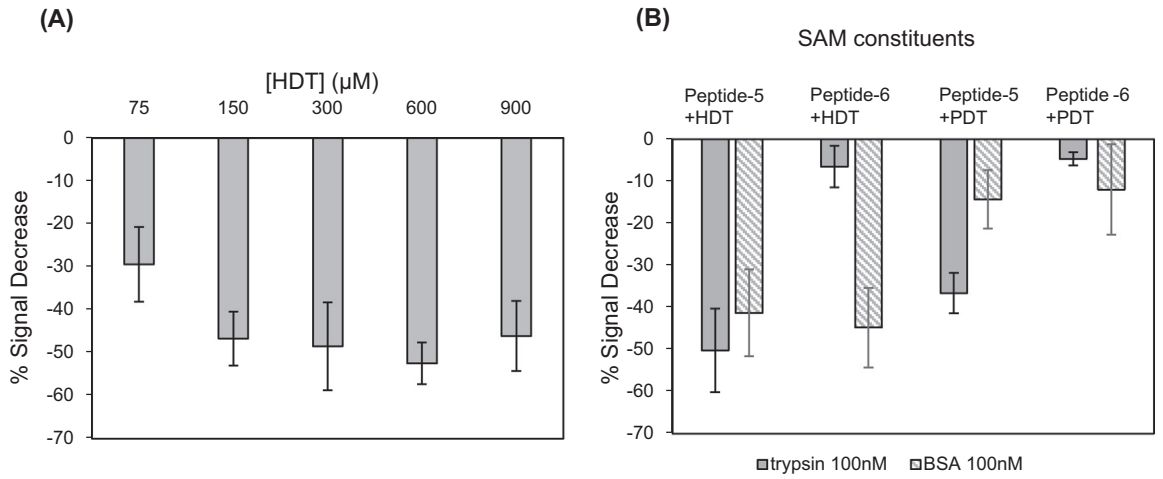

Fig. 3. (A) Comparative signals (expressed as percentage signal decrease) for trypsin 100 nM obtained for different T-SAMs prepared with 40 μM Peptide-5 and varying [HDT]. (B) Comparative signal decrease registered for T-SAMs prepared using 600 μM HDT or PDT as co-adsorbent dithiol upon the addition of trypsin (100 nM grey columns) and 100 nM BSA as a non-specific binding protein (hatched columns). Data and error bars are typically from 3 individual SAM sensing layers.

The percentage signal decrease (corrected for the maximum percentage decrease registered) measured after 70 min of incubation with solutions containing varying trypsin concentrations enabled the quantitative analysis of the logarithm of the trypsin concentration. This dose-response plot displayed an apparently sigmoidal form (Fig. 4A) for the entire measurement range (0.1–100 nM). The limit of detection (LoD), defined as the analyte concentration corresponding to 90% of the initial signal value registered, corresponded to 250 pM of trypsin. These results indicated the electrochemical biosensor readily allows measurement of trypsin in the clinically relevant range (5–15 nM for healthy individuals and 34–85 nM in the case of pancreatic conditions) (Artigas et al., 1981). Reproducibility, expressed as coefficient of variation (CV%) was found to be 4% ($n=4$) for a trypsin concentration of 100 nM. As shown in Table S2, these analytical features are comparable to those previously obtained for other trypsin sensors, with the advantage that this is "reagentless", with no need for addition of external reagents, enabling its potential use in point-of-care (PoC) devices. There is an additional obvious benefit of the negative control, which confirms the specificity of the sensor. This motivated a further selectivity study (section S3, Supplementary Data) to demonstrate the ability of the proposed sensor to give a specific and selective response to trypsin. The influence on the registered signal of potential interferents such as BSA (100 nM), casein (100 nM), dopamine (1 nM) and Ca^{2+} (1 mM) were tested. The effect of dopamine and Ca^{2+} on the signal was seen to be negligible within experimental error, whereas BSA and casein caused a degree of signal decrease; this, however, did not prevent trypsin producing a subsequently measurable signal, demonstrating the potential real-world efficacy of this sensor.

Sensing phase stability towards both successive electrochemical cycles and storage in buffer solution was also evaluated. The T-PDT-Peptide-5 SAM was immersed in a PBS solution and subjected to successive electrochemical SWV cycles. After a slight decrease (~5%) in the signal within the first 5 h, it remained essentially constant thereafter over 12 h, with the final registered value being only 10% lower than the initial one. In contrast, there was a 35% signal decrease upon 100 nM trypsin incubation, values comparable to those obtained for a freshly prepared surface not previously subjected to any electrochemical measurements. This confirmed that the signal change registered for long term experiments was not affected by any significant lack of stability of the sensing phase.

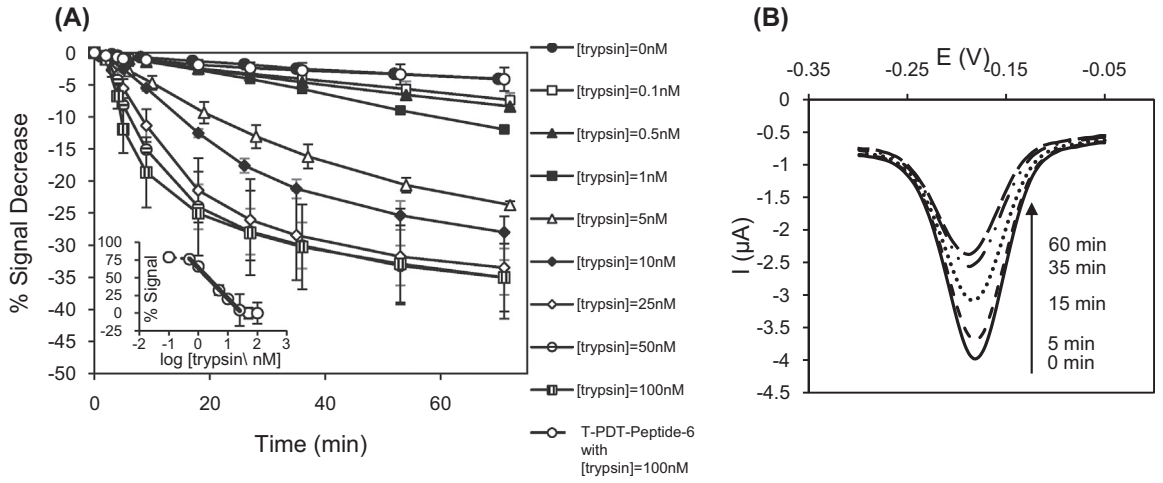

Fig. 4. Electrochemical detection of trypsin. (A) Signal-time course progression curves for T-PDT-Peptide-5 immersed in varying trypsin concentrations in 1 × PBS (0, 0.1, 0.5, 1, 5, 10, 25, 50 and 100 nM). The signal recorded upon 100 nM trypsin addition for T-PDT-Peptide-6 is also shown as a negative control. All data represent the average and errors for typically 3 individual sensing phases. Inset. Percentage signal after 70 min incubation plotted against the logarithm of the concentration of trypsin. The straight line represents the line of best fit with a correlation coefficient, $r=0.998$. (B) Typical SWV curves registered for 25 nM trypsin at different incubation times (0, 5, 15, 35 and 60 min) in 1 × PBS.

Please cite this article as: González-Fernández, E., et al., Biosensors and Bioelectronics (2015), http://dx.doi.org/10.1016/j.bios.2015.11.088

Buffer storage stability was also evaluated. T-SAMs were stored in PBS at 4 °C and the response upon trypsin addition was investigated after 3 and 7 days of storage. In both cases the sensing phases were shown to be suitable for performing a trypsin detection assay, as the signal decrease registered, 35–40% for the T-PDT-Peptide-5 SAM, was comparable to that obtained for a freshly prepared surface. Control-modified surfaces (T-PDT-Peptide-6) also registered the expected constant signal in both cases, demonstrating the desired characteristics of a negative control.

3.4.4. Kinetic analysis of enzyme cleavage

As shown previously, T-SAMs prepared with MB-tagged peptides registered a reproducible decrease in the SWV signal upon trypsin addition. Quantitative kinetic analysis of the signal decrease was developed to confirm the decrease was related to the protease activity of the trypsin and not to other events such as non-specific adsorption of the enzyme onto the modified surface or peptide probe loss from the gold surface, and to model and quantify the kinetics of the surface trypsin cleavage reaction. The details of the kinetic analysis (the proposed surface trypsin Michaelis–Menten cleavage model) are described in Section S4 (Supplementary Data, along with the data in Fig. S3 and S4) which confirms the suitability of this proposed model in describing the enzymatic cleavage taking place on the electrode surface and in extracting from the data the trypsin concentration. The registered values for K_M and k_{cat} were 28 ± 3 nM and 0.102 ± 0.004 min^{-1}, respectively. Furthermore, specificity of the signal to trypsin activity was corroborated by means of a specific trypsin inhibitor from *Glycine max* (soybean), which blocked, in real-time, the electrochemically monitored peptide cleavage.

4. Conclusions

Herein an electrochemical peptide-based biosensor for the detection of protease activity, is reported. Different probes were designed and synthesised, entailing the introduction of two modifications on a substrate peptide sequence: a redox tag (Fc or MB) and a spacer (alkyl or PEG-based chain) bearing a thiol-containing moiety for attachment to the gold surface (cysteine). We have demonstrated that MB-tagged peptides support enhanced electrochemical performance when compared to the analogous Fc-tagged peptides, characterised by a stable background and reproducible response. We propose the use of a new sensing platform consisting of a T-SAM configuration using a PEG-based dithiol as a co-adsorbent, which improved the analytical performance in terms of target accessibility and specificity, minimising non-specific adsorption of proteins. The proposed system was shown to give a quantitative response to protease concentration, fitting well to a simple Michaelis–Menten surface cleavage model and allowed measurement of trypsin activity across the entire measured concentration range without artificial restriction (e.g. assuming a linear response), with a clinically relevant LoD of 250 pM. Proteolytic specificity of the signal was further confirmed by quantitative kinetic analysis of the signal-time course, enzyme inhibition studies and the lack of response to the negative control of the equivalent D-amino acid based probes. The potential for direct measurement from real-world samples was shown by the insensitivity to selected relevant interferents. Further work will be focused on evaluating the performance of this T-SAM based sensor system when using clinical samples and the analysis of other proteases.

Acknowledgements

The authors acknowledge financial support from the EPSRC-funded Implantable Microsystems for Personalised Anti-Cancer Therapy (IMPACT) programme (Grant ref. EP/K034510/1).

Data used within this publication can be accessed at: http://dx.doi.org/10.7488/ds/365.

Appendix A. Supplementary material

Supplementary data associated with this article can be found in the online version at http://dx.doi.org/10.1016/j.bios.2015.11.088.

References

Anne, A., Chovin, A., Demaille, C., 2012. Langmuir 28, 8804–8813.
Artigas, J.M., Garcia, M.E., Faure, M.R., Gimeno, A.M., 1981. Postgrad. Med. J. 57, 219–222.
Campuzano, S., Kuralay, F., Lobo-Castañón, M.J., Bartošík, M., Vyavahare, K., Paleček, E., Haake, D.A., Wang, J., 2011. Biosens. Bioelectron. 26, 3577–3583.
Campuzano, S., Kuralay, F., Wang, J., 2012. Electroanalysis 24, 483–493.
Charles, P.T., Stubbs, V.R., Soto, C.M., Martin, B.D., White, B.J., Taitt, C.R., 2009. Sensors 9, 645–655.
Dharuman, V., Chang, B.Y., Park, S.M., Hahn, J.H., 2010. Biosens. Bioelectron. 25, 2129–2134.
Ferapontova, E.E., Olsen, E.M., Gothelf, K.V., 2008. J. Am. Chem. Soc. 130, 4256–4258.
Henry, O.Y., Sanchez, J.L., O'Sullivan, C.K., 2010. Biosens. Bioelectron. 26, 1500–1506.
Kang, D., Zuo, X., Yang, R., Xia, F., Plaxco, K.W., White, R.J., 2009. Anal. Chem. 81, 9109–9113.
Kerman, K., Mahmoud, K.A., Kraatz, H.-B., 2007. Chem. Commun. 43, 3829–3831.
Labib, M., Shipman, P.O., Martić, S., Kraatz, H.B., 2011. Analyst 136, 708–715.
Lai, R.Y., Seferos, D.S., Heeger, A.J., Bazan, G.C., Plaxco, K.W., 2006. Langmuir 22, 10796–10800.
Lai, R.Y., Plaxco, K.W., Heeger, A.J., 2007. Anal. Chem. 79, 229–233.
Li, J., Yuan, J., 2008. Oncogene 27, 6194–6206.
Liu, G., Wang, J., Wunschel, D.S., Lin, Y., 2006. J. Am. Chem. Soc. 128, 12382–12383.
Liu, Q., Wang, J., Boyd, B.J., 2015. Talanta 136C, 114–127.
Lubin, A.A., Plaxco, K.W., 2010. Acc. Chem. Res. 43, 496–505.
Martić, S., Labib, M., Shipman, P.O., Kraatz, H.B., 2011. Dalton Trans. 40, 7264–7290.
Mason, S.D., Joyce, J.A., 2011. Trends Cell Biol. 21, 228–237.
McQuistan, A., Zaitouna, A.J., Echeverria, E., Lai, R.Y., 2014. Chem. Commun. 50, 4690–4692.
Pavan, S., Berti, F., 2012. Anal. Bioanal. Chem. 402, 3055–3070.
Pazos, E., Vázquez, O., Mascareñas, J.L., Vázquez, M.E., 2009. Chem. Soc. Rev. 38, 3348–3359.
Phares, N., White, R.J., Plaxco, K.W., 2009. Anal. Chem. 81, 1095–1100.
Puiu, M., Idili, A., Moscone, D., Ricci, F., Bala, C., 2014. Chem. Commun. 50, 8962–8965.
Shah, A., Adhikari, B., Martic, S., Munir, A., Shahzad, S., Ahmad, K., Kraatz, H.B., 2015. Chem. Soc. Rev. 44, 1015–1027.
Shin, D.S., Liu, Y., Gao, Y., Kwa, T., Matharu, Z., Revzin, A., 2013. Anal. Chem. 85, 220–227.
van Kempen, L.C., de Visser, K.E., Coussens, L.M., 2006. Eur. J. Cancer 42, 728–734.
Wang, J., 2006. Biosens. Bioelectron. 21, 1887–1892.
White, R.J., Rowe, A.A., Plaxco, K.W., 2010. Analyst 135, 589–594.
Wu, J., Campuzano, S., Halford, C., Haake, D.A., Wang, J., 2010. Anal. Chem. 82, 8830–8837.
Xiao, H., Liu, L., Meng, F., Huang, J., Li, G., 2008. Anal. Chem. 80, 5272–5275.
Zhao, N., He, Y., Mao, X., Sun, Y., Zhang, X., Li, C.-z, Lin, Y., Liu, G., 2010. Electrochem. Commun. 12, 471–474.